JOURNAL OF MATERIALS SCIENCE 26 (1991) 5613–5617

Fatigue crack growth retardation in plane stress and plane strain

D. DAMRI*
University of Cambridge, Department of Materials Science and Metallurgy, Pembroke Street, Cambridge, CB2 3QZ, UK

J. F. KNOTT
University of Birmingham, School of Metallurgy and Materials, Edgbaston, Birmingham, B15 2TT, UK

The fatigue crack growth retardation phenomenon following a single peak overload applied to *thick* and *thin* SEN bend specimens has been studied for a low carbon structural steel. Fatigue tests were performed under a constant load ratio of 0.6, constant stress intensity range of 10 MPa m$^{1/2}$ and a constant overload ratio of 2.5. An immediate increase followed by a transient retardation in the fatigue crack growth rate, due to the applied overload, was observed for the *thick* specimen but complete crack arrest was obtained for the *thin* specimen. The immediate increase in the fatigue crack growth rate following the single peak overload in the *thick* specimen was attributed to the coincidence of monotonic fracture modes.

1. Introduction

Crack closure is often cited as the primary fatigue crack growth retardation mechanism following the application of a single peak overload [1, 2, 3]. Such a phenomenon is often attributed to be an "edge effect" and is thus associated with a predominantly plane stress state. It is normal practice to isolate and analyse such an effect by employing *thin* specimens [3]. Under constant stress intensity range (ΔK) and load ratio (R) conditions a fatigue crack, in a single edge notch (SEN) bend specimen, propagates at a faster fatigue crack growth rate (da/dN) in a *thick* testpiece than in a *thin* testpiece, but in SEN tension specimens a *slant mode* of fatigue fracture in the *thin* testpiece can produce more rapid crack propagation than that in a *thick* testpiece [4]. Such a phenomenon has been attributed to an antiplane strain mode of deformation.

The present work shows the differences in transient fatigue crack growth response in *thick* and *thin* SEN bend specimens subjected to the same loading and overloading conditions.

2. Experimental procedure

The material used for the research was a low carbon structural steel (0.18C, 1.5Mn, 0.04S). The material was received as 20 mm plate and all specimens were machined with the longitudinal axis in the rolling direction. Specimens were ground and stress relieved at 650 °C for 2 h in a vacuum furnace to remove any residual machining stresses. The final dimensions of the specimens were $w = b = 18$ mm for the *thick* testpieces, and $w = 18$ mm, $b = 3$ mm for the *thin* testpieces (where w and b represent the width and thickness, respectively). A starter notch was machined to a depth of 5 mm. The tensile strength and the yield strength of the steel were 450 MPa and 240 MPa, respectively.

Initially the fatigue crack growth characteristics in the Paris and threshold regimes for *thick* ($b = 18$ mm) and *thin* ($b = 3$ mm) specimens were obtained at a constant load ratio of $R = 0.6$ ($R = K_{min}/K_{max}$, where K_{max} and K_{min} represent the maximum and minimum stress intensity, respectively). Single peak overload tests were performed on *thick* and *thin* SEN specimens in a four point bend loading configuration, using a closed loop servohydraulic machine interfaced with a micro-computer. All tests were performed under sinusoidal loading at a frequency of 40 Hz in laboratory air conditions.

Overload fatigue tests for both *thick* and *thin* specimens were performed at a load ratio ($R = K_{min}/K_{max}$) of $R = 0.6$ and a baseline stress intensity range ($\Delta K_b = K_{max} - K_{min}$) of $\Delta K_b = 10$ MPa m$^{1/2}$. The overload ratio (OLR) was defined as $(K_{ol} - K_{min})/(K_{max} - K_{min})$ where K_{ol} defines the overload stress intensity. The overload ratio was kept at a constant value of 2.5 for both *thick* and *thin* specimens.

3. Results and discussion

The fatigue crack growth curves in Fig. 1 clearly show that growth rates are faster in the *thick* ($b = 18$ mm) testpiece than in the *thin* ($b = 3$ mm) testpiece (e.g. at $\Delta K = 10$ MPa m$^{1/2}$, da/dN in the *thick* specimen is

* Author to whom all correspondence should be addressed.

0022–2461/91 $03.00 + .12

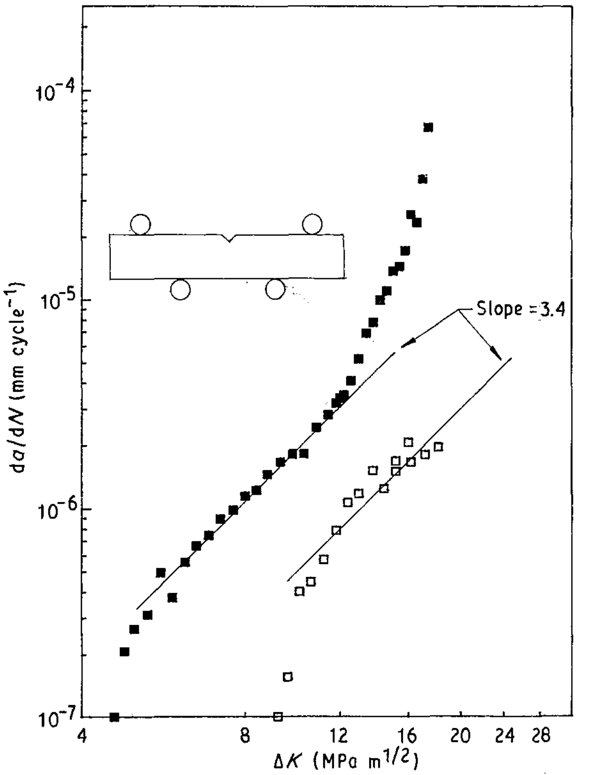

Figure 1 Fatigue crack growth curves for *thick* and *thin* SEN specimens under four point bend at a load ratio of 0.6. (■) *Thick* specimen (b = 18 mm) and (□) *thin* specimen (b = 3 mm).

2×10^{-6} mm cycle^{-1} and in the *thin* testpiece is 4×10^{-7} mm cycle^{-1}). Both specimens are represented in the linear growth regime by approximately the same slope corresponding to the exponent $m = 3.4$ in the Paris equation

$$\frac{da}{dN} = C(\Delta K)^m$$

where C represents the Paris constant. The extent of the Paris regime for the *thick* and *thin* specimens is given by the limits $6\ \mathrm{MPa\,m^{1/2}} \leqslant \Delta K \leqslant 13\ \mathrm{MPa\,m^{1/2}}$, and $10.5\ \mathrm{MPa\,m^{1/2}} \leqslant \Delta K \leqslant 16\ \mathrm{MPa\,m^{1/2}}$, respectively. The threshold stress intensity range, ΔK_{th}, was experimentally determined and corresponded to a growth rate of 10^{-7} mm cycle^{-1}. For *thick* and *thin* specimens, both at a load ratio of 0.6, ΔK_{th} was found to be 4.8 MPa m$^{1/2}$ and 9.2 MPa m$^{1/2}$, respectively. It is worth noting that Ritchie *et al.* [4] observed growth rates comparable with those in the present work for *thick* and *thin* SEN bend specimens made from a high nitrogen mild steel.

The fatigue crack growth rate response due to the application of a single peak overload on a *thick* SEN bend specimen is shown in Fig. 2. Prior to the overload a fatigue crack was grown at $R = 0.6$ and $\Delta K_b = 10$ MPa m$^{1/2}$ resulting in a growth rate of 2×10^{-6} mm cycle^{-1}. The application of a single peak overload (OLR = 2.5) caused severe blunting of the crack tip and an incremental crack extension of ~ 0.18 mm. From SEM observations, as shown in Fig. 4, the application of an overload corresponded to a ductile "stretch zone" forming in a striation across the specimen's thickness. Both void coalescence with the blunted crack tip and void–void coalescence were observed on the fatigue surface. No fracture modes were observed in the predominantly plane stress regions, up to 1.8 mm from each of the specimens side faces (see diagram inset in Fig. 2). The lack of void

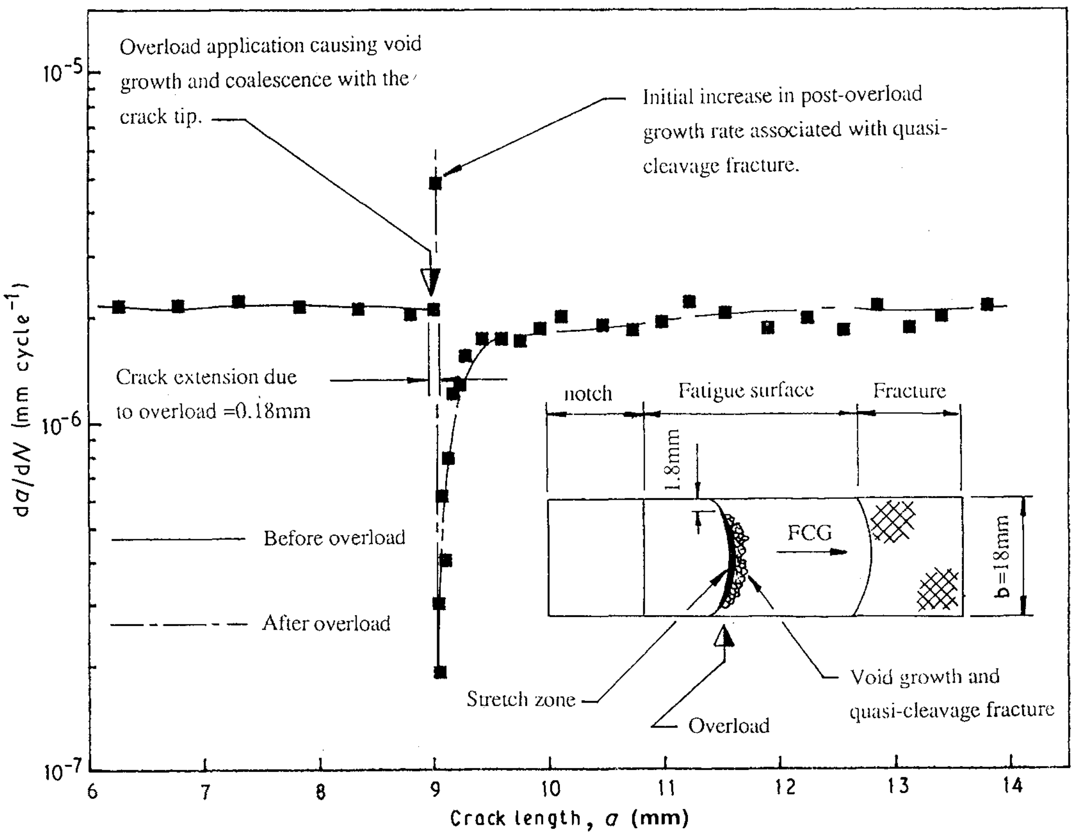

Figure 2 Effect of a single peak overload on growth rate for *thick* SEN bend specimen (R = 0.6, ΔK_b = 10 MPa m$^{\frac{1}{2}}$, OLR = 2.5).

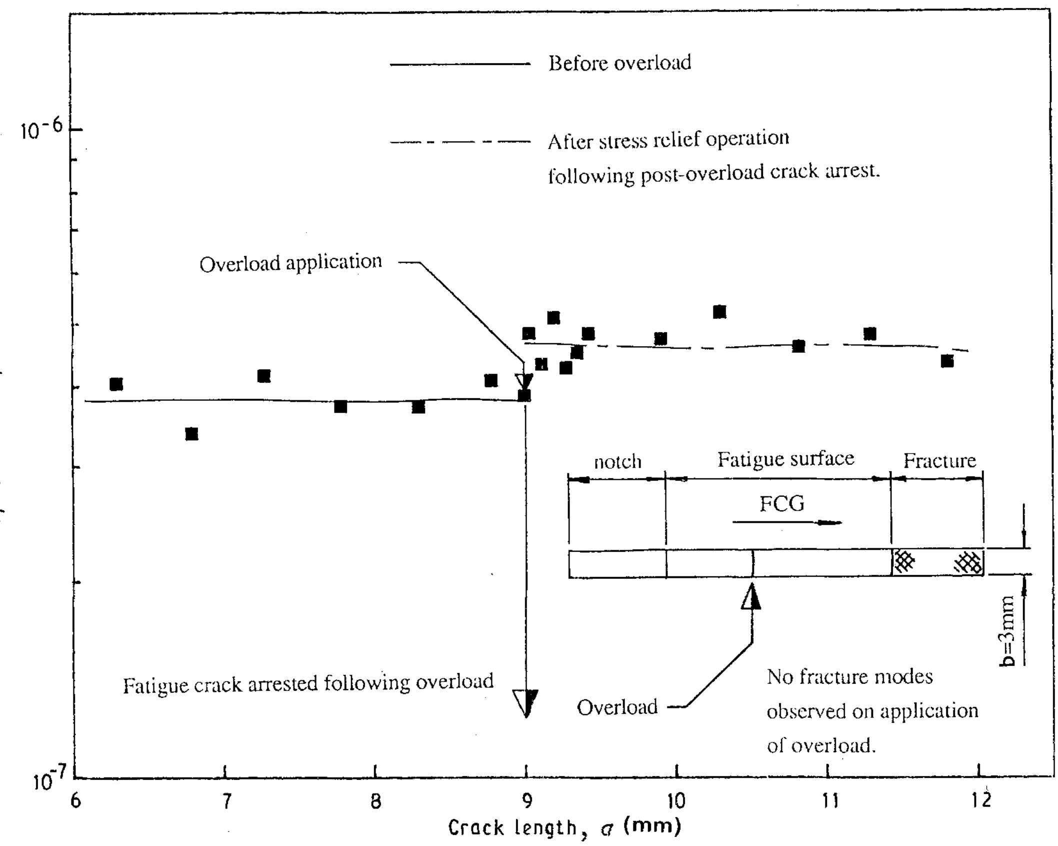

Figure 3 Effect of a single peak overload on growth rate for *thin* SEN bend specimen ($R = 0.6$, $\Delta K_b = 10\ \mathrm{MPa\,m^{\frac{1}{2}}}$, OLR = 2.5).

growth in the plane stress region is attributed to the low hydrostatic stress state. Upon refatiguing the initially faster post-overload growth rate was attributed to quasi-cleavage fracture which was observed on the fatigue surfaces, as shown by Fig. 5. The growth rate then dropped to a minimum value approaching $\sim 10^{-7}$ mm cycle^{-1}. Recovery to the steady state growth rate occurred within ~ 0.25 mm. No crack closure, measured from a load/clip gauge displacement plot, was detected either before or immediately after the application of the overload.

The fatigue crack growth rate response due to a single peak overload in a *thin* SEN bend specimen is shown in Fig. 3. A pre-overload fatigue crack was grown at $R = 0.6$, $\Delta K_b = 10\ \mathrm{MPa\,m^{1/2}}$, resulting in a steady state growth rate of 4×10^{-7} mm cycle^{-1}.

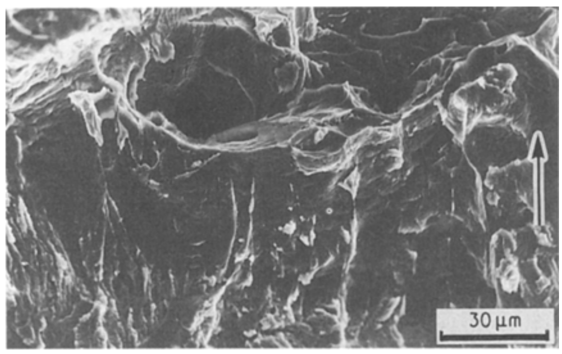

Figure 5 Cleavage facet on fatigue surface of *thick* specimen, associated with increased growth rates found upon re-fatiguing immediately after application of a single peak overload. ($R = 0.6$, $\Delta K_b = 10\ \mathrm{MPa\,m^{\frac{1}{2}}}$, OLR = 2.5). Arrow indicates direction of crack growth.

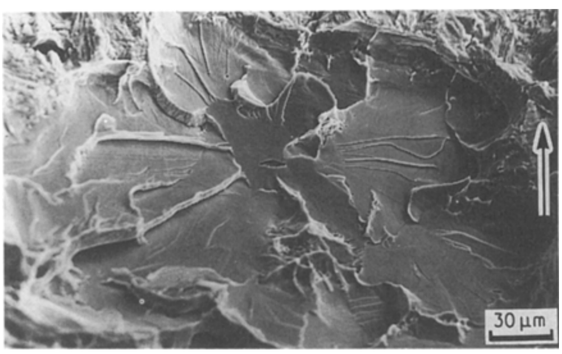

Figure 4 Stretch zone and void formation due to a single peak overload in a *thick* specimen ($R = 0.6$, $\Delta K_b = 10\ \mathrm{MPa\,m^{\frac{1}{2}}}$, OLR = 2.5). Arrow indicates direction of crack growth.

From SEM observations the fatigue surface appeared as small angular facets oriented at 45° through the thickness as shown in Fig. 6. The application of a single peak overload (OLR = 2.5) resulted in complete crack arrest, i.e. no crack growth was detected (within the resolution of the potential drop crack monitoring system) within a period of 1.5×10^6 cycles. Fatigue crack growth was resumed after a stress relief heat treatment at 650 °C for 2 h in a vacuum furnace. Since blunting of the crack tip had occurred on application of the overload, the stress relief operation would tend to indicate that the mechanism of arrest should be attributed to the generation of a residual compressive stress field ahead of the fatigue crack tip. Although blunting of the crack tip had occurred, microscopic

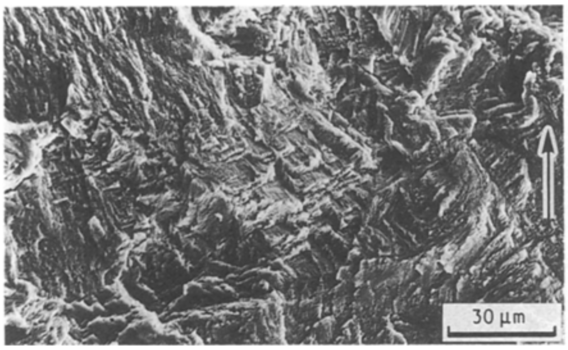

Figure 6 Fatigue surface morphology for *thin* specimen at $R = 0.6$, $\Delta K_b = 10\ \mathrm{MPa\,m^{\frac{1}{2}}}$. Arrow indicates direction of crack growth.

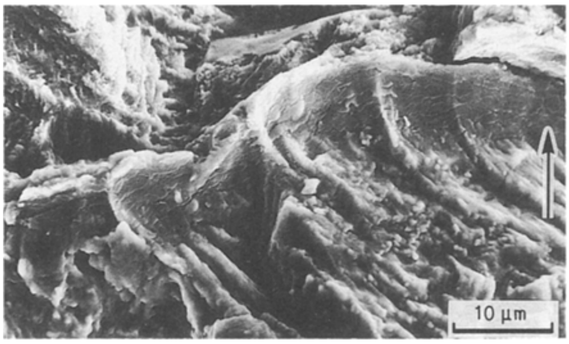

Figure 7 Striation formation due to a single peak overload in a *thin* specimen ($R = 0.6$, $\Delta K_b = 10\ \mathrm{MPa\,m^{\frac{1}{2}}}$, OLR = 2.5). Arrow indicates direction of crack growth.

SEM examination revealed only a single striation across the specimen's thickness as shown in Fig. 7. No monotonic fracture modes, cleavage or void growth, were evident on the fatigue surface.

The absence of monotonic fracture modes in the *thin* specimen thus represent conditions similar to those in the plane stress region of the *thick* specimen. The crack arrest condition experienced by the *thin* specimen is an extreme condition of the transient retardation phenomenon experienced by the plane stress region in the *thick* specimen and is responsible for the bowing of the overloaded fatigue crack in the *thick* specimen.

The previous experiments compared fatigue crack growth behaviour under constant ΔK conditions. It is of interest to examine comparative behaviour at constant $\mathrm{d}a/\mathrm{d}N$. This was achieved by growing a fatigue crack in a *thin* specimen, under a constant $\Delta K = 15\ \mathrm{MPa\,m^{1/2}}$, which corresponded to a growth rate of $2 \times 10^{-6}\ \mathrm{mm\,cycle^{-1}}$. From visual examination this loading condition produced a square mode of fatigue crack growth. SEM observations showed that a ductile striation fatigue growth mechanism predominated. The fatigue crack surface appeared rougher, compared to the fatigue surface from the *thin* testpiece at $\Delta K = 10\ \mathrm{MPa\,m^{1/2}}$, with a high degree of microvoiding and shear cracking around MnS inclusion particles, as shown in Fig. 8. This was similar to the fatigue surface on the *thick* specimen, at $\Delta K = 10\ \mathrm{MPa\,m^{1/2}}$ and $\mathrm{d}a/\mathrm{d}N = 2 \times 10^{-6}\ \mathrm{mm\,cycle^{-1}}$. In a fatigue test performed on a *thin* testpiece, when

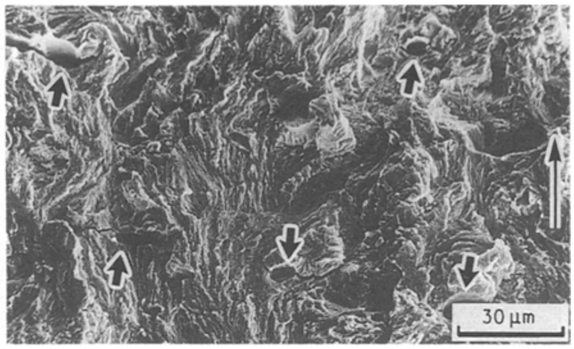

Figure 8 Fatigue surface morphology for *thin* specimen, exhibiting micro-voiding and shear cracking (indicated by small arrows) at $R = 0.6$, $\Delta K_b = 15\ \mathrm{MPa\,m^{\frac{1}{2}}}$. Arrow indicates direction of crack growth.

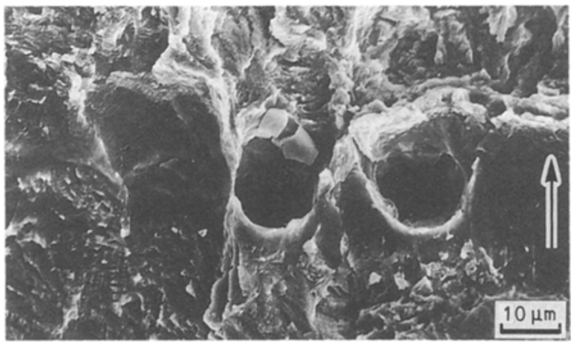

Figure 9 Stretch zone and void formation in a *thin* specimen due to an increase in ΔK from 10 to $15\ \mathrm{MPa\,m^{\frac{1}{2}}}$, at $R = 0.6$. Arrow indicates direction of crack growth.

increasing ΔK from $10\ \mathrm{MPa\,m^{1/2}}$ to $15\ \mathrm{MPa\,m^{1/2}}$, a ductile stretch zone resulted involving void growth and coalescence with the blunted fatigue crack tip as shown by Fig. 9. These observations made on *thin* specimens may be used to deduce that the plane stress zone, in the *thick* specimen, has the potential to sustain void growth given a sufficiently large overload.

4. Conclusions

An experimental study has been performed on *thick* and *thin* SEN bend specimens made from a low carbon structural steel in an attempt to ascertain the retardation phenomenon encountered on application of a single peak overload. The following conclusions have been reached:

1. On application of a single peak overload on a fatigue crack in a *thick* specimen, void growth followed by cleavage fracture is observed followed by a transient retardation in the fatigue crack growth rate.
2. Following the application of a single peak overload on a fatigue crack in a *thin* specimen, complete crack arrest results. No monotonic fracture modes were observed on the fatigue surface. The *thin* specimen, subjected to the same stress intensity range, load ratio and overload ratio as the *thick* specimen, seems to represent the fatigue crack growth phenomenon in the plane stress region of the *thick* specimen.

3. The fatigue surface of a *thin* specimen, grown at the same *growth rate* as that in a *thick* specimen, exhibited a similar fractographic appearance indicating similar modes of crack growth.

Acknowledgements

The authors would like to thank British Rail, Derby and the SERC for financial support to D. Damri. They are also grateful to Professor D. Hull for the provision of research facilities.

References

1. C. S. SHIN and N. A. FLECK, *Fatigue Fract. Engng Mater. Struct.* **9** (1987) 379–93.
2. C. M. WARD-CLOSE, A. F. BLOM, and R. O. RITCHIE, *Eng. Frac. Mech.* **32** (1989) 613–38.
3. N. A. FLECK, ASTM STP 924 (1988) pp. 157–83.
4. R. O. RITCHIE, R. F. SMITH and J. F. KNOTT, *Metal Science* **9** (1975) 485–92.

Received 6 July 1990
and accepted 31 January 1991